

# Transforming Condition-based Data Signatures into Functional Failure Signatures

James P. Hofmeister  
Ridgetop Group, Inc.  
3580 West Ina Road  
Tucson, AZ 86741  
520-742-3300x107  
hoffy@ridgetopgroup.com

Douglas L. Goodman  
Ridgetop Group, Inc.  
3580 West Ina Road  
Tucson, AZ 86741  
520-742-3300  
doug@ridgetopgroup.com

Ferenc Szidarovszky  
Ridgetop Group, Inc. 3580  
West Ina Road  
Tucson, AZ 86741  
520-742-3300  
szidarka@gmail.com

**Abstract**—This paper describes the transformation of conditioned-based data (CBD) signatures into functional-failure signatures (FFS) that are particularly amenable to processing by prediction algorithms. CBD signatures comprise feature data (FD) that creates a signature that is highly correlated to degradation. Degradation proceeds from the onset of damage to a level of damage at which a component, and its assembly, no longer functions within operational specifications: functional failure occurs. A CBD-based feature signature correlates a change in value ( $dP$ ) of a parameter of interest ( $P_0$ ) as degradation progresses. This paper presents a theory that each failure mode generates a characteristic degradation signature:  $g(dP, P_0)$ . Further, a feature signature can be transformed into a dimensionless ratio to create a fault-to-failure progression (FFP) signature:  $FFP = \{f(FD_i, FD_0)g(dP_i, P_0)\}$  that, when solved in terms of another ratio, creates a degradation progression signature (DPS):  $DPS = \{dP_i/P_0\} = \{f(FFP_i)\}$ .

Absent noise, a DPS is a linear straight-line transfer curve that is easily transformed into a functional-failure signature (FFS) that is particularly amenable to processing to produce prognostic information in support of Prognosis for Health Monitoring/Management (PHM): (1) an FFS approaches an ideal straight-line transfer curve as noise is ameliorated and/or mitigated; (2) has negative values in the absence of degradation; (3) has positive values below 100 when there is degradation below a defined level of functional failure; and (4) has values at or above 100 when the level of degradation is at or above a level defined as functional failure. Even in the presence of noise and feedback effects, and even when the rate of degradation is nonlinear, a DPS is still a very linear transfer curve.

The authors present seven different families of increasing signatures and decreasing signatures that can be represented by seven degradation-signature models that, coupled with models for defining a level of function failure, are used to transform CBD-based signature data into FFS data.

## TABLE OF CONTENTS

1. INTRODUCTION.....	1
2. PROGNOSTICS.....	1
3. SIGNATURES.....	3
4. DPS AND FSS MODELING .....	6
5. CONDITIONING AND HEURISTIC APPROACH.....	11
6. SUMMARY AND CONCLUSION .....	12
APPENDICES.....	12
A. DERIVATION OF A DPS MODEL .....	12

B. DERIVATION OF A DPS FAILURE LEVEL .....	12
C. FFS NONLINEARITY CALCULATIONS .....	12
ACKNOWLEDGEMENTS .....	13
REFERENCES.....	13
BIOGRAPHY.....	14

## 1. INTRODUCTION

This paper briefly reviews prognostics: its purpose and benefits, including the acquisition of data in support of reliable condition-based monitoring (RCM) using condition-based data (CBD). A concept is introduced that CBD signatures that have characteristic curves related to changes in value(s) as a parameter degrades. A switched-mode power supply (SMPS) having a filter capacitance that degrades is used as an example to illustrate how a characteristic CBD signature is transformed into a fault-to-failure progression (FFP) signature; how that FFP signature is transformed into a degradation-progression signature (DPS); and how that DPS is transformed into a functional-failure signature (FFS) that is particularly amenable for processing by prediction algorithms to produce prognostic information such as remaining useful life (RUL) and state-of-health (SoH) estimates.

Next, seven sets of models are presented to generate CBD signatures, their characteristic curves, their related models for transforming CBD signature data into DPS data, and then into FFS data. The models are used to transform signatures from one form to other forms. Plots are included to illustrate the usefulness of such transforms.

The paper ends with a summary. Details on derivation and modeling are included in an appendix.

## 2. PROGNOSTICS

Prognostics is an ability to accurately detect and report future failures in systems. The purpose of prognostics is to detect degradation and create prognostic information such as estimates of SoH and RUL of systems for the following benefits: (1) provide advance warning of failures; (2) minimize unscheduled maintenance; (3) predict the time to perform preventive replacement; (4) increase maintenance

cycles and operational readiness; (5) reduce sustainment costs by decreasing inspection, inventory, and down-time costs; and (6) increase reliability by improving the design and logistic support of existing systems [1, 2, 3].

Referring to Figure 1, prognostics includes data acquisition (DA) by sensors (S) and data manipulation (DM) by processing within a sensor framework. Additional processing within a feature-vector framework to include detection, isolation, and identification. That state detection (SD) produces feature data (FD) that are condition indicators that comprise leading indicators of failure (signatures). Health assessment (HA) and prognostic assessment (PA) are performed within a prediction framework. The sensor framework, feature-vector framework, prediction framework, and a control and data flow framework comprise a prognosis subsystem within a prognosis and health management (PHM) system. [4, 5]

Figure 2 shows approaches to prognostics: three classical approaches – model-driven, data-driven, and hybrid-driven –

and a CBD approach that often employs analysis and modeling techniques such as reliability modeling, physics-of-failure (PoF) analysis, and failure-mode effects analysis (FMEA). The reliability of a CBM approach for prognostics is dependent on reliable and accurate prognostic information, which depends on how accurately the sensing system collects and conditions data and how accurately that data is processed by prediction algorithms in producing prognostic information. Curvilinear CBD that is reliably and accurately transformed into linearized data is very useful for processing to produce reliable and accurate prognostic information.

The focus of this paper is transforming condition-based data (CBD) signatures into fault-to-failure progression (FFP) signatures, degradation-progression signatures (DPS), and functional-failure signatures (FFS) [6, 7, 8]. FFS data as input into a prediction framework, such as that shown in Figure 3, increases the reliability and accuracy of prognostic information such as RUL and SoH estimates.

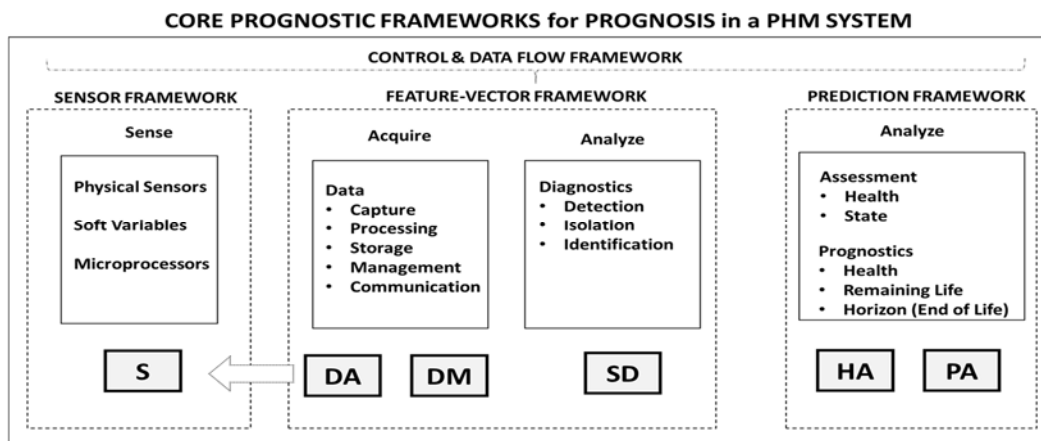


Figure 1. Core prognostic frameworks in a PHM system (after [4])

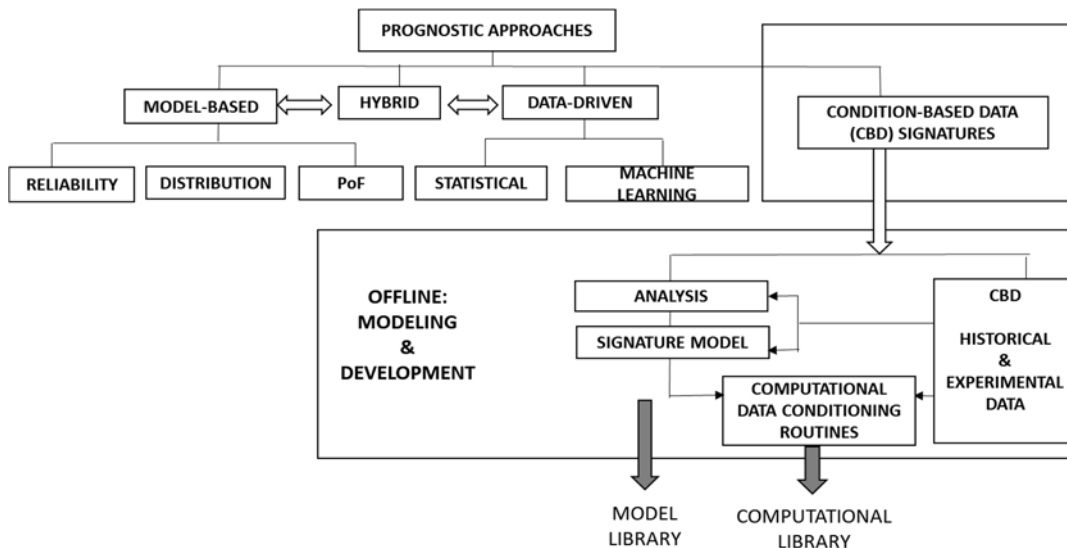


Figure 2. Classical and CBD approaches to prognostics (after [1])

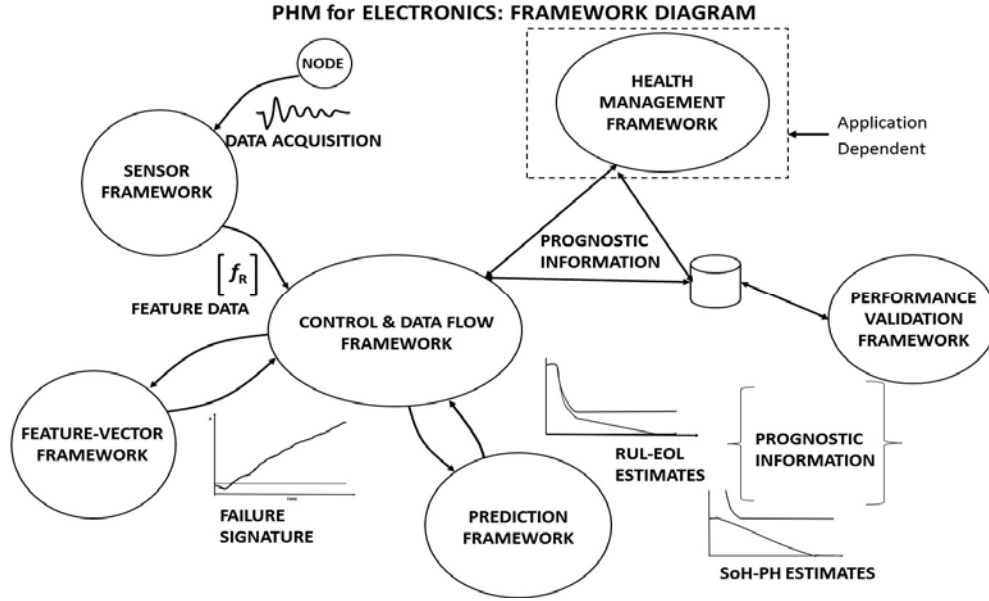


Figure 3. Example PHM system showing core frameworks (after [5])

### 3. SIGNATURES

A signature characterizes a feature of interest, such as feature data ( $FD$ ) that changes in amplitude over a period of time:  $T = \{t_m, t_{m+1}, \dots, t_{m+n}\}$ . Amplitude refers to a characteristic value such as voltage, current, resistance, force, energy and so on that changes as the magnitude of damage/degradation increases over time:

$$FD = \{FD_m, FD_{m+1}, \dots, FD_{m+n-1}, FD_{m+n}\} \quad (1)$$

Four sets of signature data of interest related to signals and prognostic processing are identified: CBD (in terms of  $FD$ ), FFP, DPS, and FFS. An FFP signature is a transform of a CBD signature to reduce modeling complexity and a DPS signature is a transform of an FFP signature to further reduce modeling complexity and to increase the reliability and accuracy of prognostic information. An FFS is a transform of either an FFP or a DPS signature that is particularly amenable to processing by prediction algorithms because of commonality of FFS signatures and values.

#### Condition-based Data (CBD) Signature

A sensor is located at a node of prognostic interest to monitor and collect data. An example is the output node of a switch-mode power supply (SMPS): the output voltage (Figure 4) comprises multiple types of features and noise, including damped-ringing responses, switching noise from power transistors, ripple voltage, pulse-width modulator effects, effects of voltage and current regulation and feedback, and background noise. Sensors can be designed to support the isolation and extraction of leading indicators of failure, such as a damped-ringing response (Figure 5) seen in the output of a SMPS. [6, 7, 9 – 12]

$$\mathbf{V} = CBD_1 + CBD_2 + \dots + CBD_n + N_1 + N_2 + N_m \quad (2)$$

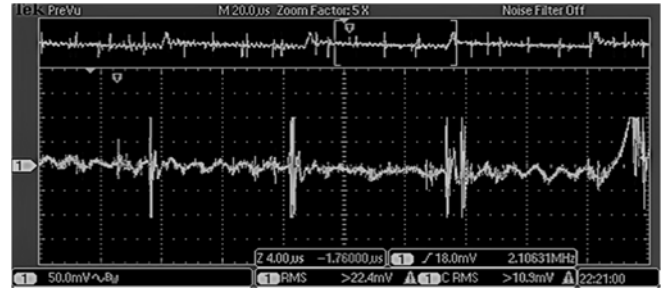


Figure 4. Voltage at the output node of an SMPS

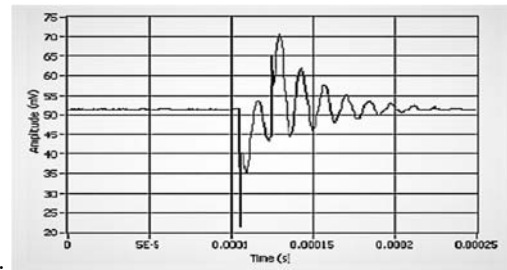


Figure 5. Damped-ringing response

Signal processing isolates, extracts, conditions, and transforms data to create a particular  $FD$  value, such as the resonant frequency of a damped-ringing response. A collection of  $FD$  points over time is a CBD signature: an example of which is shown in Figure 6.

An idealized damped-ringing response can be modeled as multiple features of interest including the following: a DC voltage  $V_{DC}$ , a response amplitude  $A_R$ , a dampening time constant  $\tau$ , a frequency  $\omega$ , and a phase shift  $\phi$ ; [10, 11]

$$V_0 = V_{DC} + A_R \{ \exp(-t/\tau) \} \{ \cos(\omega t + \phi) \} \quad (3)$$

PoF analysis shows that as the filter capacitance of an SMPS

degrades, the resonant frequency changes: [10, 11]

$$\omega \approx \omega_0 \sqrt{C_0 / (C_0 - \Delta C)} \quad (4)$$

Then from  $f = \omega / 2\pi = FD$  [10],

$$FD = FD_0 \sqrt{C_0 / (C_0 - \Delta C)} \quad (5)$$

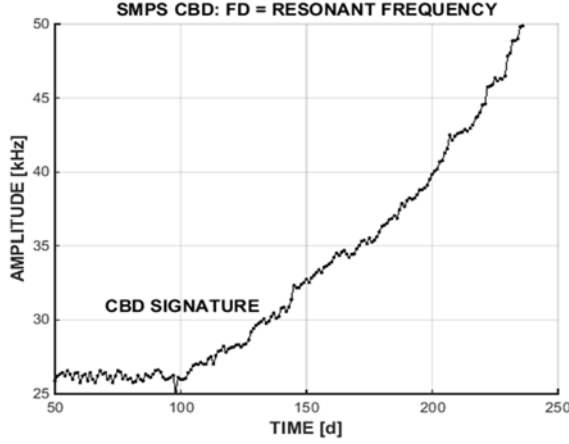


Figure 6. Resonant frequency over time

#### Fault-to-Failure Progression (FFP) Signature

An FFP signature (see Figure 7) is a collection of normalized, dimensionless data obtained by transforming FD points starting with a particular point,  $m$ , and ending at a final point,  $m+n$ :

$$FFP = \{FFP_m, FFP_{m+1}, \dots, FFP_{m+n-1}, FFP_{m+n}\} \quad (6)$$

Where the FFP point for an  $i$ -th FD point is given by the following in which  $NM$  is noise margin ( $NM/FD_0$  in Figure 7). [7]

$$FFP_i = (FD_i - FD_0 - NM) / FD_0 \quad (7)$$

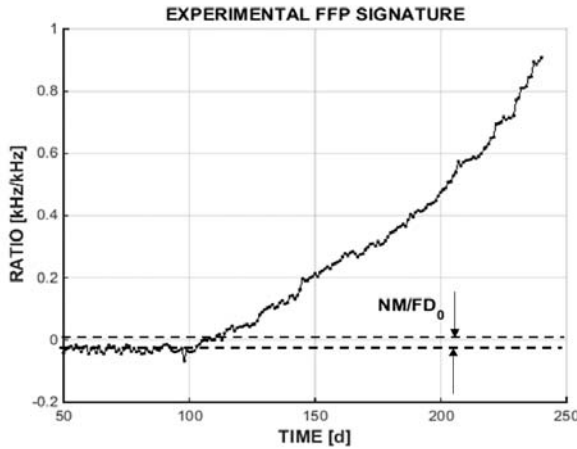


Figure 7. FFP transformed from CBD in Figure 6

Compared to CBD signatures, FFP signatures are more amenable to prognostic processing because normalized, dimensionless data simplifies modeling and processing.

Values at or below zero indicate an absence of detectable degradation and values greater than zero indicate a presence of degradation. Functional failure occurs when degradation reaches a defined level: for example, 0.60 for one application and 0.70 for another application.

#### FFP-based Functional-failure signature (FFS)

Since functional failure occurs when degradation reaches a defined FFP value, a prediction algorithm that processes FFP signature data needs application-specific knowledge such as a failure threshold value and/or FFP model. To address that consequence, we introduce the FFS signature produced by dividing FFP signature data by a defined failure level (FL) and multiplying the result by 100:

$$FFS_{FFP} = (FFP/FL)100 \quad (8)$$

While such FFS data has the same, generally curvilinear, characteristic shape as the FFP signature it is based on, the signature simplifies processing by prediction algorithms (see Figure 8):

- $FFS_i \leq 0$  no degradation
- $0 < FFS_i < 100$  degradation
- $FFS_i \geq 100$  functionally failed

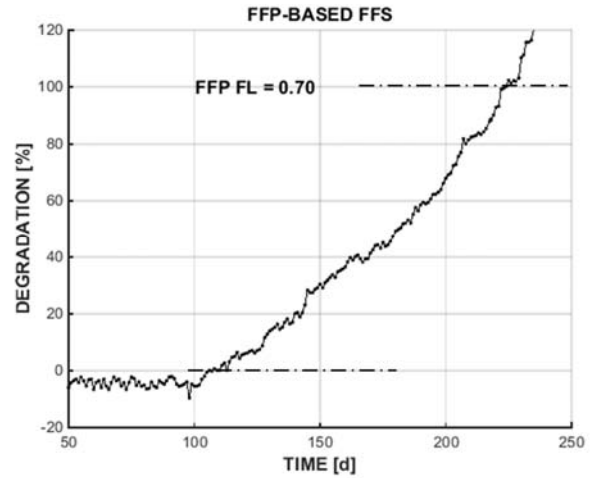


Figure 8. FFS based on the FFP in Figure 6: FL = 0.7

A disadvantage of FFP-based FFS data is the signature is generally curvilinear: it has the same characteristic curve as the original CBD signature as seen by comparing Figure 6 and Figure 8.

#### Degradation Progression Signature (DPS)

A DPS is a collection of transformed FFP signature points: it is a function of a change in value,  $dP$ , of a parameter of interest  $P_0$ : (1) when there is no degradation, the value of the parameter is unchanged and  $dP = 0$ ; (2) as degradation progresses, the magnitude of  $dP$  increases:

$$DPS = \{DPS_m, DPS_{m+1}, \dots, DPS_{m+n}\} \quad (9)$$

$$DPS_i = dP_i/P_0 \quad (10)$$

From Eq. (5) and Eq. (7), for our exemplary SMPS, and using Eq. (9) and Eq. (10) as shown in Appendix A, we get the following:

$$FD_i = FD_0 (\sqrt{P_0/(P_0 - dP_i)}) \quad (10)$$

Solving for  $dP_i/P_0$  in Eq. (10) leads to the following (see Appendix A):

$$DPS_i = dP_i/P_0 = 1 - (FD_0/FD_i)^2 \quad (11)$$

A major advantage of DPS data is that its characteristic curve is defined by  $dP_i/P_0$  and when that is linear, which is often the case, the DPS is linear. Even when  $dP_i/P_0$  is not linear, a DPS signature curve is more linear than its underlying FFP signature. Figure 9 plots the **DPS** from using Eq. (11) to transform the **FFP** plotted in Figure 7.

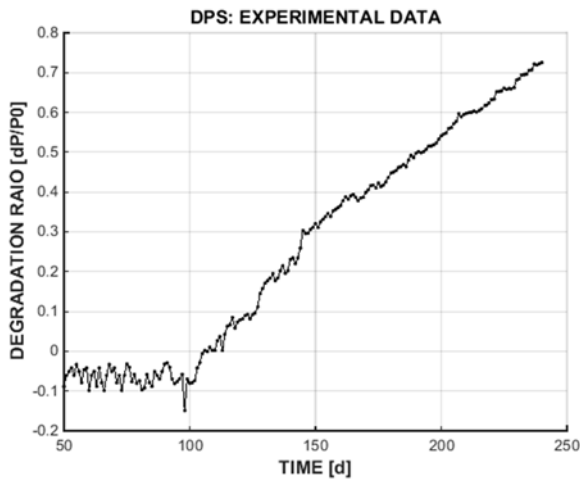


Figure 9. DPS from the FFP signature in Figure 7

#### DPS-based FFS

FFS data based on DPS data is functionally the same as FFS data based on FFP signature data:

$$FFS_{DPS} = (DPS/FL_{DPS})100 \quad (12)$$

To ensure equivalency, the failure level for DPS data must be derived from the FFP-based failure level. For this example (see Appendix B),

$$FL_{DPS} = 1 - (1/(1 + FL_{FFP}))^2 \quad (13)$$

As example and referring back to Figure 7, suppose we defined functional failure to occur at FFP = 0.70, then from Eq. (13) we calculate the equivalent DPS-based failure level to be 0.65 with plotted FFS results shown in Figure 10:

$$FL_{DPS} = 1 - (1/1.70)^2 = 0.65$$

#### Model Verification

It is important to verify models used in a PHM system: simulate models against experimental and/or actual fielded data. When FFS data is input to prediction algorithms in your PHM system, the resultant prognostic information needs to meet the accuracy, convergence, and reliability requirements. Model verification starts with a general form:

$$FD = FD_0 f(dP, P_0) \quad (14)$$

where the degradation function,  $f(dP, P_0)$ , depends on, for example, the component that is degrading and the failure mode. and the physics-of-failure. The degradation function for the example of Eq. (10) is the following:

$$f(dP, P_0) = \sqrt{P_0/(P_0 - dP_i)}$$

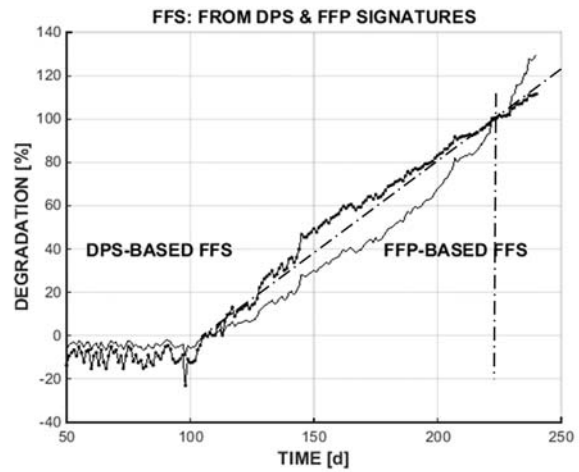


Figure 10. FFS plots showing equivalent failure levels

Compare signatures—One verification step is to compare ideal model signatures to those of actual and/or experimental data. For example, Figure 11 shows there is a difference between the plots of the exemplary CBD signature and the plots of an ideal CBD from Eq. (10):

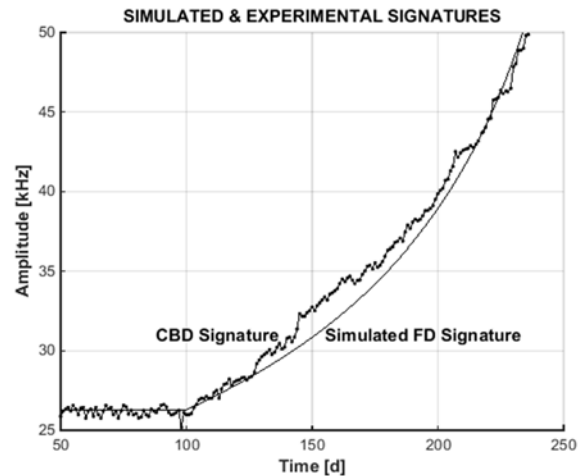
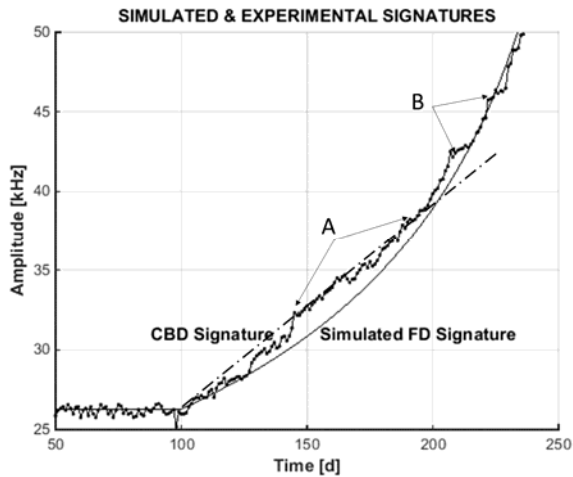


Figure 11. FFS plots showing equivalent failure levels

*Explain variations*—Another verification step is to explain variations/differences between what is obtained and what was expected: then either accept and/or remedy any variation. For example, referring to Figure 12, the major difference between the plots of the experimental data and the simulated (ideal) data was determined to be (A) the effects of the regulation feedback loop in the power supply and (B) step-like changes resulting from a test-bed method for injecting faults (loss of capacitance). This comparison explains the nonlinearity of the DPS-based FFS and an ideal, straight-line FFS – the ‘dot-dash’ straight line in Figure 10.



**Figure 12. Comparison of actual and simulated CBD**

*Non-linearity*—Another verification step is to evaluate the nonlinearity of an FFS signature compared to an ideal straight line. We define FFS nonlinearity (FNL) as a measure of the deviation between an actual FFS and an ideal FFS (see Figure 13): very much like an integral nonlinearity (INL) assessment of an analog-to-digital data converter (ADC) or transducer output transfer curve [13,14,15].

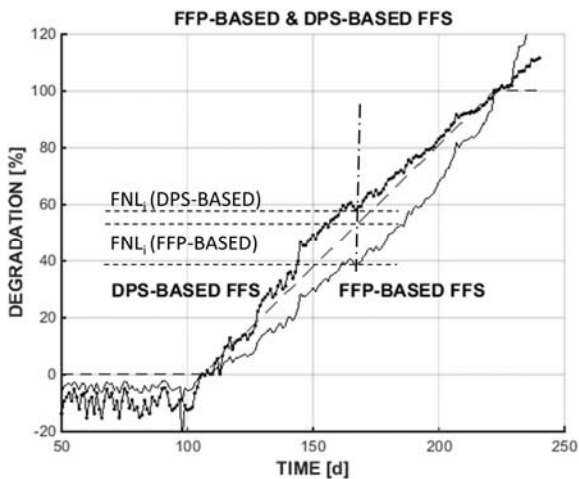


**Figure 13. FNL for DPS- and FFP-based FFS data**

A point-by-point FNL is a measurement of the error between an actual FFS value and the ideal FFS value at that point in time and a total FNL error ( $FNL_E$ ) provides an assessment of the nonlinearity of the FFS curve (see Figure 14 and Appendix C).

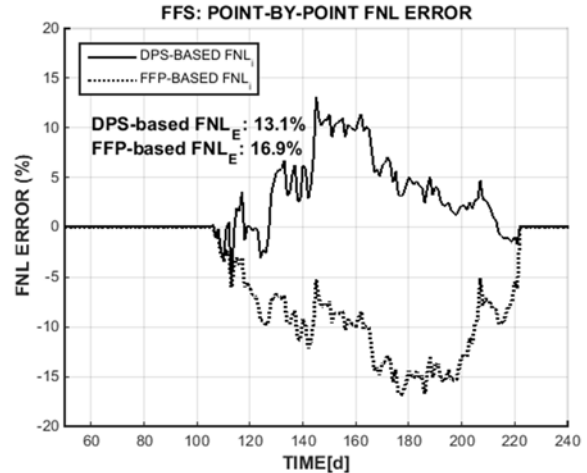


**Figure 14. Example of point-by-point FNL for FFS data**

#### 4. DPS AND FFS MODELING

Degradation-related signatures result from failure modes that can be modeled as power functions or exponential functions.

##### *Degradation Functions*

To transform signatures from one form to another, the authors developed seven sets of degradation functions (see Table 1): five are power functions and two are exponential functions, which have either increasing or decreasing amplitudes – constant signatures are only applicable in the sense that they indicate the absence of degradation. Signatures having decreasing amplitudes are transformed to a complementary, increasing amplitude signature and degradation model. Degradation signatures are further classified by whether the signature has a decreasing or increasing slope angle as degradation progresses: a linear, straight-line degradation signature is a special case that is classified as having a constant slope angle. The slope angle is the arc between a tangent to the curve and the horizontal axis. Sample plots of degradation functions and their DPS transforms are shown in Figure 15 through Figure 21.

**Table 1. Degradation Functions**

Function Set and Type	Decreasing Amplitude	Increasing Amplitude
Set 1: Power-function	$-(dP_i/P_0)^n$	$(dP_i/P_0)^n$
Set 2: Power-function	$1 - [1/(1 - dP_i/P_0)]^n$	$[1/(1 - dP_i/P_0)]^n - 1$
Set 3: Power-function	$[1/(1 + dP_i/P_0)]^n - 1$	$1 - [1/(1 + dP_i/P_0)]^n$
Set 4: Power-function	$1 - (1 + dP_i/P_0)^n$	$(1 + dP_i/P_0)^n - 1$
Set 5: Power-function	$(1 - dP_i/P_0)^n - 1$	$1 - (1 - dP_i/P_0)^n$
Set 6: Exponential-function	$1 - \exp(dP_i/P_0)$	$\exp(dP_i/P_0) - 1$
Set 7: Exponential-function	$\exp(-dP_i/P_0) - 1$	$1 - \exp(-dP_i/P_0)$

**Table 2. Transform Models**

Increasing FFP	Increasing DPS	DPS-based FFS
$\{FFP\} = \{(FD_i - FD_0)/FD_0\}$	$\{DPS\} = \{(dP_i/P_0)\}$	$\{FFS_{DPS}\} = (\{DPS\}/FL_{DPS})100$
$FD_i = FD_0 g(dP_i, P_0)$	$dP_i/P_0 = f(FFP_i)$	$FL_{DPS} = h(FL_{FFP})$
$g(dP_i, P_0)$	$f(FFP_i)$	$h(FL_{FFP})$
$(dP_i/P_0)^n$	$(FFP_i)^{1/n}$	$(FL_{FFP})^{1/n}$
$[1/(1 - dP_i/P_0)]^n - 1$	$1 - 1/(FFP_i + 1)^{1/n}$	$1 - 1/(FL_{FFP} + 1)^{1/n}$
$1 - [1/(1 + dP_i/P_0)]^n$	$1/(1 - FFP_i)^{1/n} - 1$	$1/(1 - FL_{FFP})^{1/n} - 1$
$(1 + dP_i/P_0)^n - 1$	$(FFP_i + 1)^{1/n} - 1$	$(FL_{FFP} + 1)^{1/n} - 1$
$1 - (1 - dP_i/P_0)^n$	$1 - (1 - FFP_i)^{1/n}$	$1 - (1 - FL_{FFP})^{1/n}$
$\exp(dP_i/P_0) - 1$	$\ln(FFP_i + 1)$	$\ln(FL_{FFP} + 1)$
$1 - \exp(-dP_i/P_0)$	$\ln(1/(1 - FFP_i))$	$\ln(1/(1 - FL_{FFP}))$

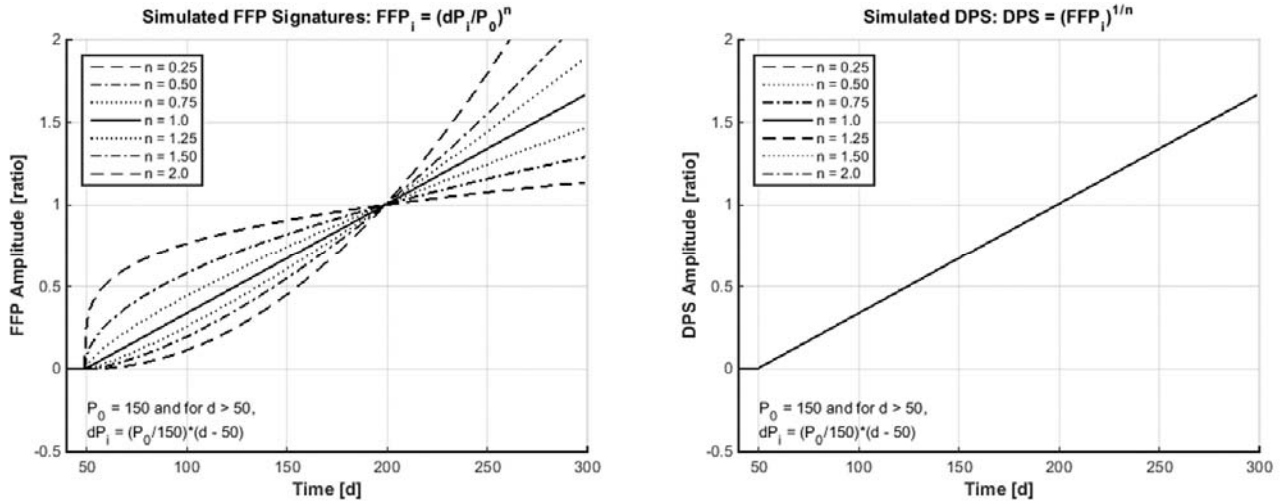


**Figure 15. Example FFP and DPS plots for  $f(dP_i, P_0) = (dP_i/P_0)^n$**

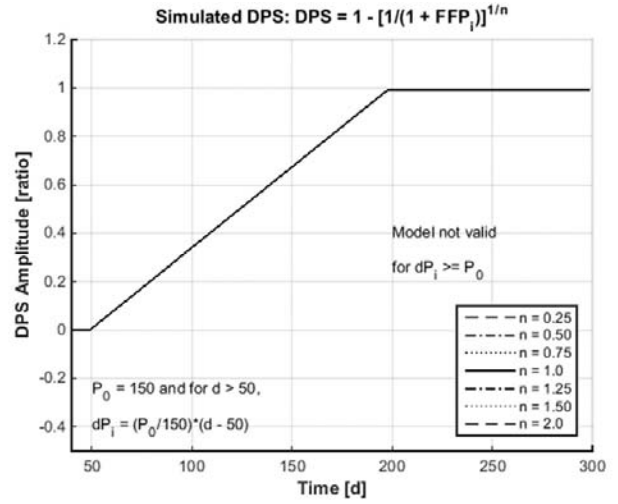
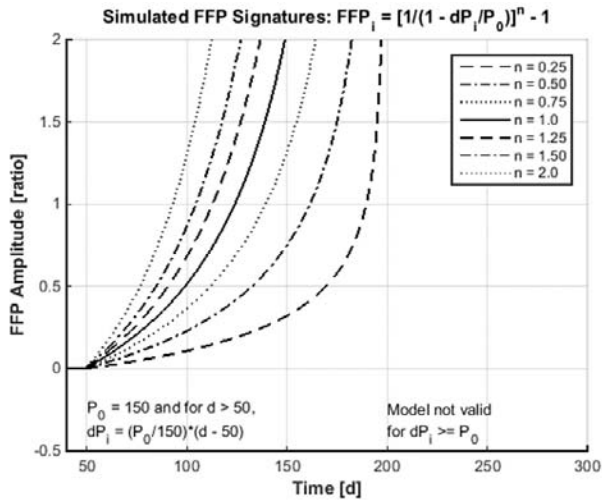


Figure 16. Example FFP and DPS plots for  $f(dP_i, P_0) = [1/(1 - dP_i/P_0)]^n - 1$

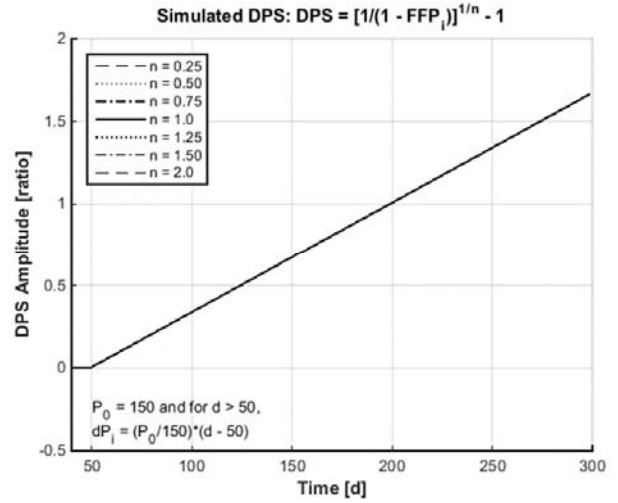
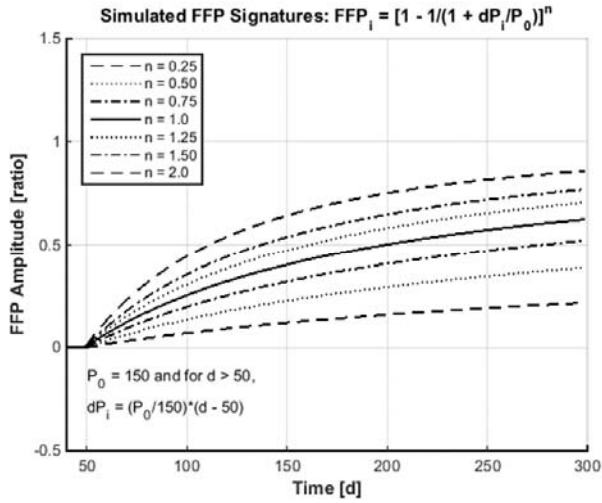


Figure 17. Example FFP and DPS plots for  $f(dP_i, P_0) = 1 - [1/(1 + dP_i/P_0)]^n$

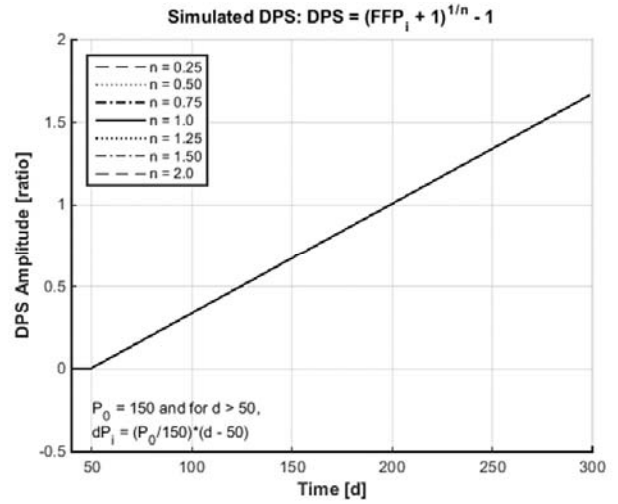
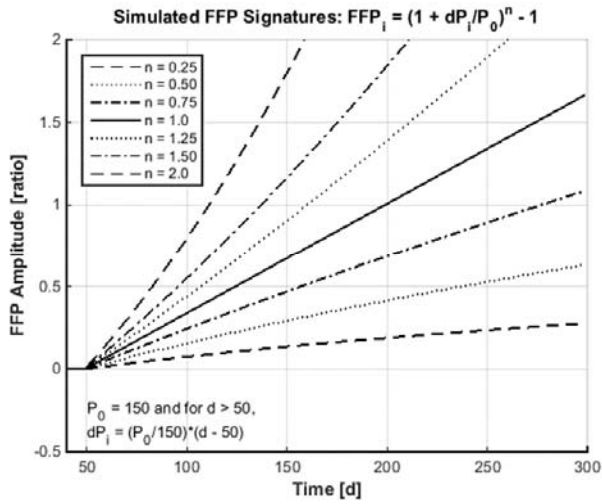


Figure 18. Example FFP and DPS plots for  $f(dP_i, P_0) = (1 + dP_i/P_0)^n - 1$

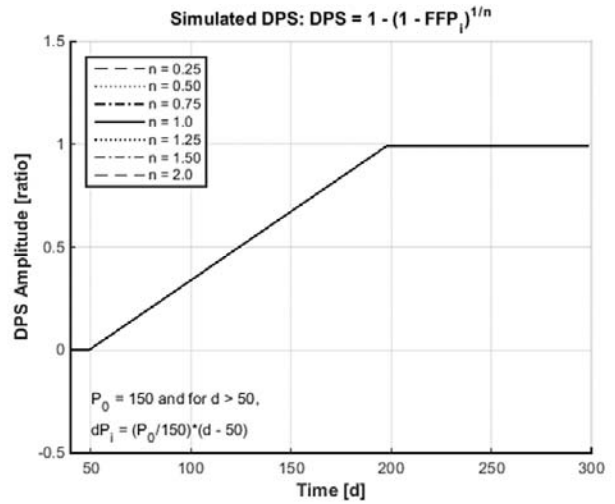
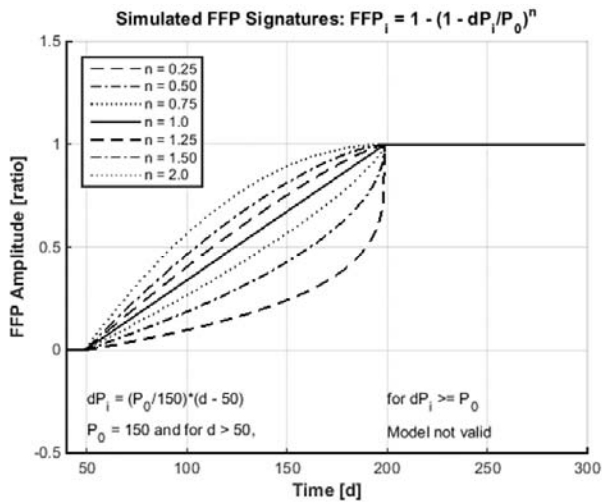


Figure 19. Example FFP and DPS plots for  $f(dP_i, P_0) = 1 - (1 - dP_i/P_0)^n$

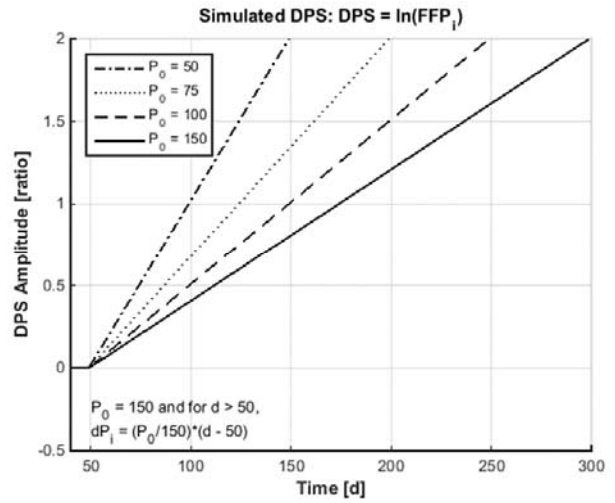
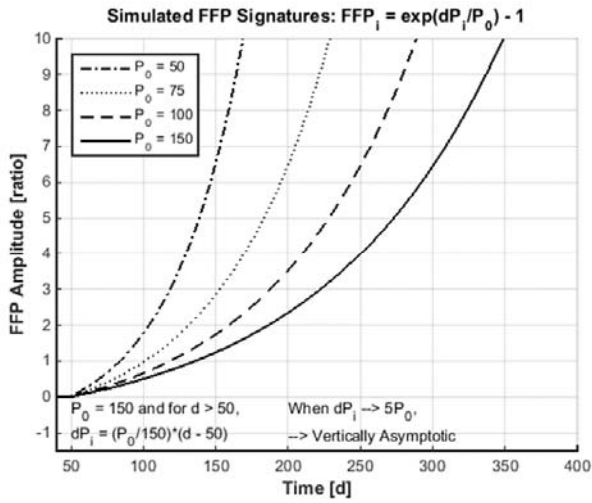


Figure 20. Example FFP and DPS plots for  $f(dP_i, P_0) = \exp(dP_i/P_0) - 1$

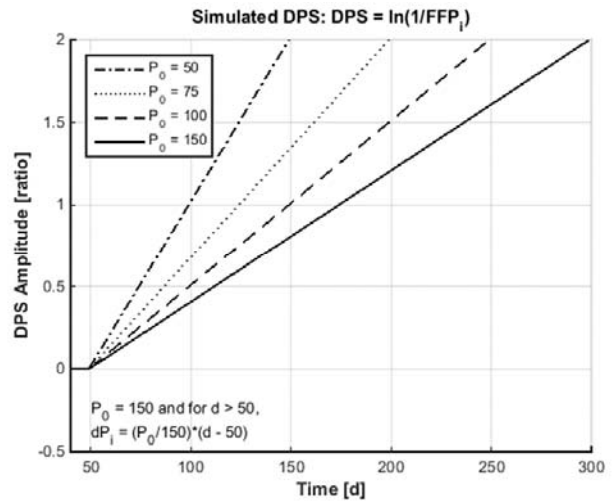
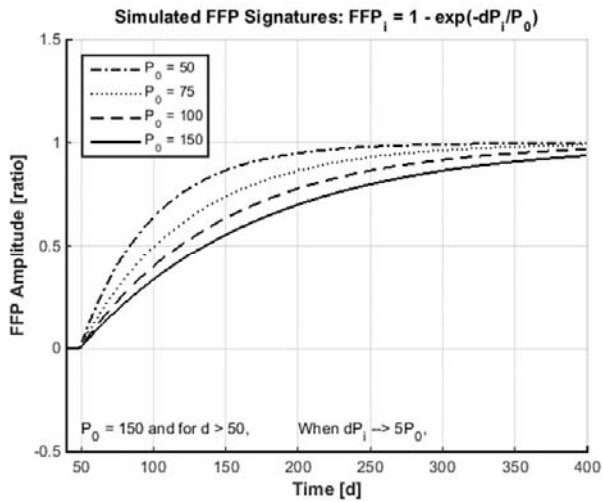


Figure 21. Example FFP and DPS plots for  $f(dP_i, P_0) = \exp(dP_i/P_0) - 1$  and  $f(dP_i, P_0) = 1 - \exp(-dP_i/P_0)$

### Modeling CBD Signatures to FFS Data

A general procedure has been developed to use the seven sets of degradation functions to transform CBD signatures into DPS-based FFS data to be input to prediction algorithms (see Figure 22).

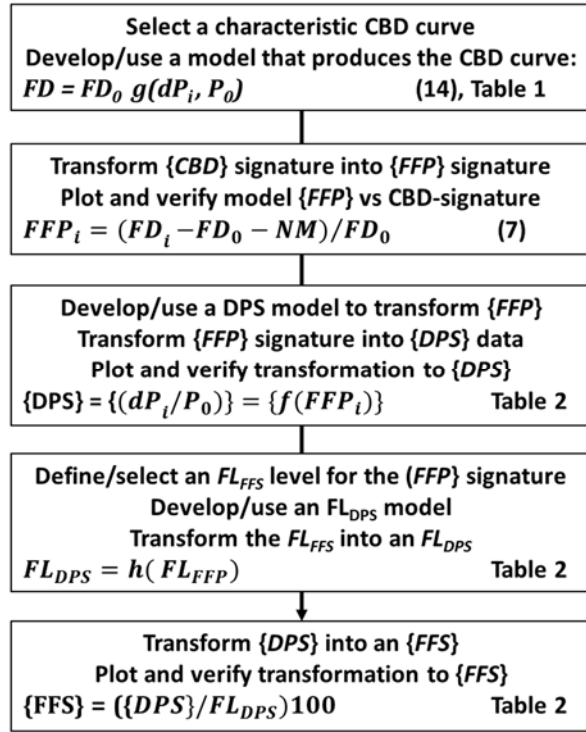
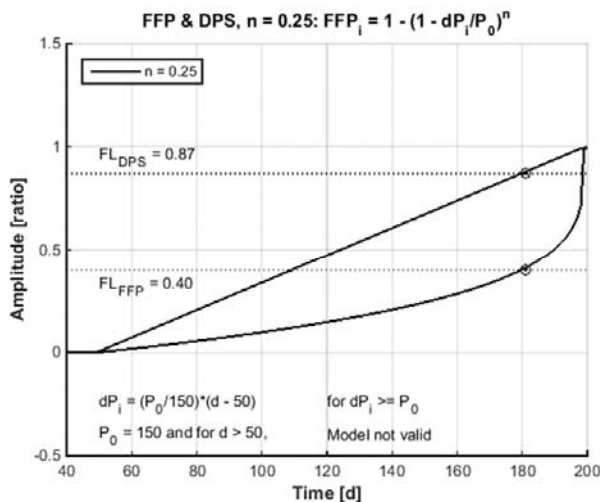


Figure 22. Procedure for transforming CBD signatures

### Functional Failure Signature (FFS)

To create a set of DPS points, use a generalized form of Eq. (11) and a set of models from column 1 and column 2 of Table 1 :

$$\{DPS\} = \{(dP_i/P_0)\} \text{ and } dP_i/P_0 = f(FFP_i)$$



Then select/define a threshold FFP value that defines functional failure: a level at which the component, assembly, and/or system is no longer operating within specifications,

$$FL_{FFP} = FFP_i = \text{threshold for functional failure}$$

Then transform  $FL_{FFP}$  into  $FL_{DPS}$  using a generalized form of Eq. (13) and a model from column 3 of Table 2:

$$FL_{DPS} = h(FL_{FFP})$$

This transform is necessary to ensure that regardless of whether an FFS is based on an FFP signature or on a DPS, functional failure occurs at same point in time. For example, the plots in Figure 23 illustrate that regardless of whether the FFP results from a power or exponential function of degradation, functional failure occurs, as expected, at the same point in time.

A next step is to use Eq. (12) and  $FL_{DPS}$  to transform a DPS signature into an FFS signature:

$$\{FFS_{DPS}\} = (\{DPS\}/FL_{DPS})100$$

Figure 24 shows the FFS plots for the two DPS and two FFP plots in Figure 23. Notable observations are the following: (1) the DPS-based FFS plots are more linear compared to the FFP-based FFS plots; (2) all four FFS plots have the same units of measure (percent in amplitude and days in time); (3) functional failure occurs when an FFS is at 100 percent; and (4) the two FFP-based FFS plots are similar, but not exactly the same.

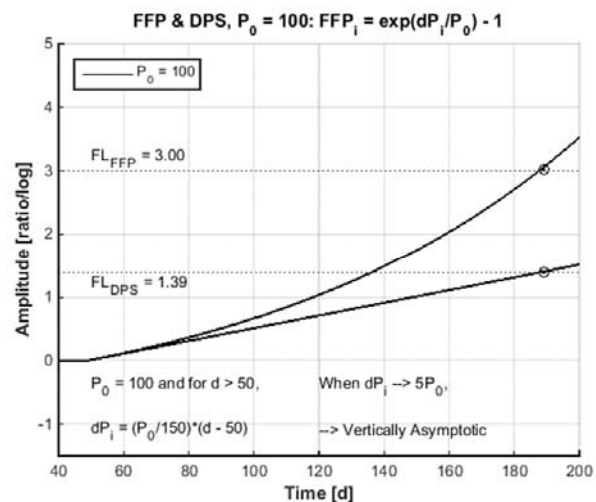


Figure 23. Plots for  $FL_{FFP}$  (selected) and  $FL_{DPS}$  (calculated): functional failure occurs at same point in time

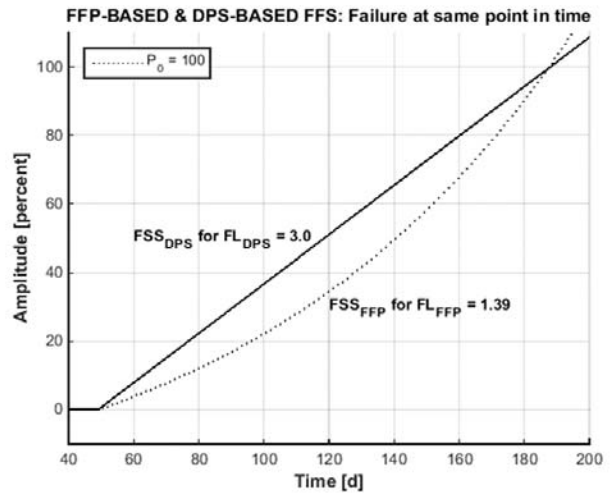
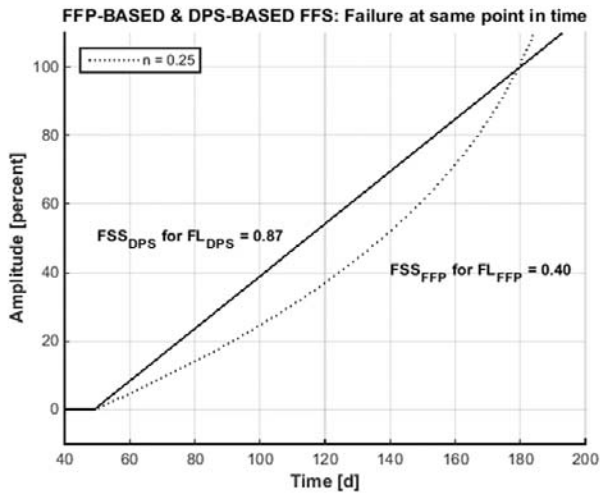


Figure 24. FSS plots for  $FL_{FFP}$  (selected) and  $FL_{DPS}$  (calculated): functional failure occurs at same point in time

#### Data Point by Data Point Transformation

An important note: all of the data transforms are successively performed one data point at time: there is no prior knowledge of any future data point at any step in the transformation of CBD to FFP to DPS to FSS:

For a first data point ( $i = 1$ ): (1) transform  $CBD_i$  to  $FFP_i$ ; then (2) transform  $FFP_i$  to  $DPS_i$ ; then (3) transform  $DPS_i$  to  $FSS_i$ ; then (4) input  $FSS_i$  to your prediction algorithm. Repeat for the second and all subsequent data points ( $i=2, 3, \dots$ ).

### 5. CONDITIONING AND EMPIRICAL APPROACH

To improve results, apply a data smoothing technique to the FFP signature and/or adjust the noise margin. For example, Figure 7 indicates a smaller noise margin of 0.6 instead of 0.7 could be used, resulting in the plot shown in Figure 25. Because regulation with feedback results in non-ideal square-root function ( $n=1/2$ ), it is suitable to use  $n=1$  instead of  $n=1/2$  to transform the smoothed FFP signature data into an improved DPS signature data as seen in Figure 26.

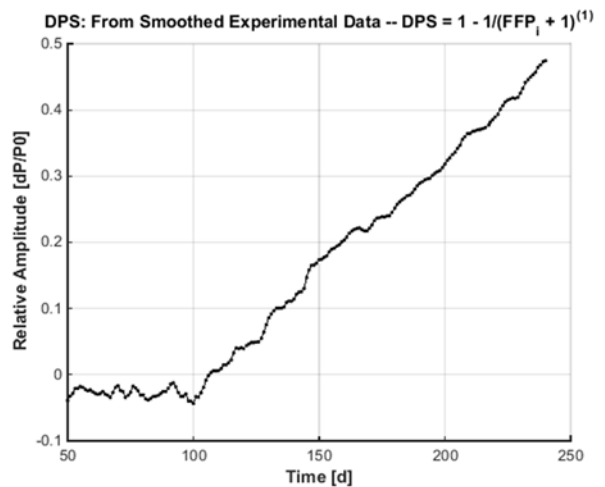


Figure 26. Conditioned DPS – contrast with Figure 9

Figure 27 and Figure 28 illustrate the improvements that are achievable by conditioning the FFP signature and by empirically changing the power when transforming the FFP signature.

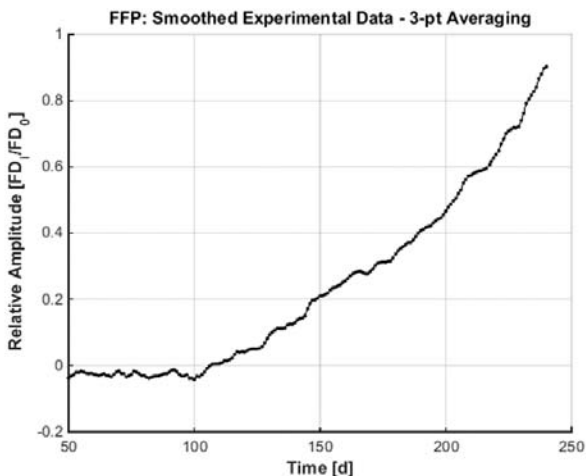


Figure 25. Conditioned FFP – contrast with Figure 7

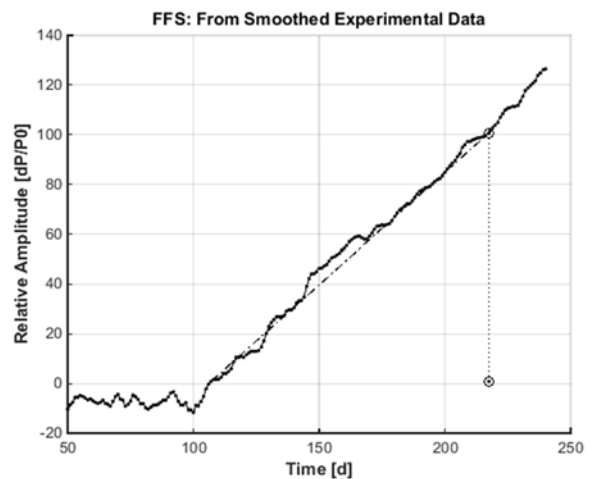
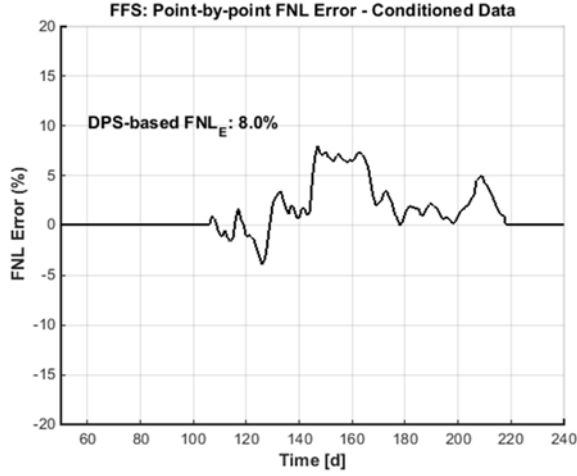


Figure 27. Conditioned FFS – contrast with Figure 13



**Figure 28. Non-linearity for conditioned FFS – contrast with Figure 14**

Most importantly, the improved DPS results in an FFS with less non-linearity: the maximum non-linearity has been reduced to 8.0 percent compared to the original 16.9 for an FFS based on the FFP and the 13.1 for an FFS based on the unconditioned DPS (refer back to Figure 14). Even when a prediction algorithm does not employ sophisticated prediction methods and techniques, the small non-linearity in the conditioned FFS data is likely to produce accurate prognostic information.

## 6. SUMMARY

In this paper an exemplary prognostic system is reviewed: a set of core frameworks, classical and CBD approaches to handle data, and control and data flow. Then a concept of signatures is introduced with a set of examples to illustrate that CBD contains features that can be extracted as FD to create an FFP signature, which can be further transformed into DPS data and then into FFS data – one data point at time. An ideal FFS, as a transfer curve for producing prognostic information, is a straight line progressing from 0 percent or less (no degradation) to 100 percent or higher (functionally failed). Next a method is introduced to evaluate non-linearity of FSS data (FNL): that method is based one used for evaluating the nonlinearity of data converters.

A procedure for transforming CBD signatures into FFS data is introduced: included is a set model functions developed for that purpose. Plots of the model functions showed that for ideal CBD (FFP) data, the resulting DPS and FSS curves are linear.

The paper is concluded by using the original example data to illustrate how data conditioning and evaluating experimental data leads to a empirical approach for transforming signatures: choose a set of model functions to transform signatures, then use a value for power or exponent that is suitable for the application and which results in a more linear FFS.

## APPENDICES

### A. DERIVATION OF A DPS MODEL

Beginning with the general model for a point in an FFP signature, Eq. (7),

$$FFP_i = (FD_i - FD_0)/FD_0$$

to which we apply a model for an  $FD$  of interest, such as that for resonant frequency of a damped-ringing response of an SMPS: Eq. (5),

$$FD_i = FD_0 (\sqrt{C_0/(C_0 - \Delta C_i)})$$

Let  $P_0 = C_0$  and  $dP_i = \Delta C$ , then we get Eq. (10)

$$FD_i = FD_0 (\sqrt{P_0/(P_0 - dP_i)})$$

Which leads to

$$P_0/(P_0 - dP_i) = (FD_i/FD_0)^2$$

$$P_0/(FD_i/FD_0)^2 = P_0 - dP_i$$

and re-arranging terms,

$$P_0(FD_0)^2/(FD_i)^2 = P_0 - dP_i$$

$$(FD_0/FD_i)^2 = (P_0 - dP_i)/P_0 = 1 - dP_i/P_0$$

we get Eq. (11)

$$DPS_i = dP_i/P_0 = 1 - (FD_0/FD_i)^2$$

### B. DERIVATION OF A DPS FAILURE LEVEL

Although any DPS value can be chosen as a failure level, such a failure level should be based on an FFP-based failure level:

$$FL_{FFP} = FFP_i$$

then from Eq. (7) for failure at defined value of  $FD_i$  and ignoring the noise margin,

$$FL_{FFP} = (FD_i - FD_0)/FD_0$$

so that

$$FD_i - FD_0 = FD_0 FL_{FFP}$$

$$FD_i = FD_0 FL_{FFP} + FD_0$$

$$FD_0/FD_i = 1/(FL_{FFP} + 1)$$

and from Eq. (11),

$$FL_{DPS} = 1 - (1/(1 + FL_{FFP}))^2 \quad (13)$$

### C. FFS NONLINEARITY CALCULATIONS

Calculating FSS nonlinearity is a post-processing type of operation using FFS data because it is necessary to first

calculate the total time between the point in time of the onset of degradation and the point in time when functional failure occurs:

$$TTF = t_{FAILURE} - t_{ONSET}$$

then for each point in the set  $\{FFS_i\}$ , we create an ideal point,

$$IDEAL\_FFS_i = 100 (t_i - t_{ONSET})/TTF$$

and calculate point-by-point nonlinearity,

$$FNL_i = FFS_i - IDEAL\_FFS_i$$

and calculate total nonlinearity,

$$FNL_E = \max(\text{abs}(\{FNL_i\}))$$

where ‘max’ is a maximum function and ‘abs’ is an absolute-value function. Figure 14 is an example of FNL plots.

#### ACKNOWLEDGEMENTS

The authors thank Naval Air, Naval Sea, U.S. Army, U.S. Air Force, and NASA research centers for their support and funding of multiple projects that led to the results described and shown in this paper.

#### REFERENCES

- [1] Pecht, M. (2008) *Prognostics and Health Management of Electronics*. Hoboken, NJ: John Wiley & Sons.
- [2] Kumar, S. and Pecht, M. (2010) “Modeling Approaches for Prognostics and Health Management of Electronics,” *International Journal of Performability Engineering*, Vol. 6, No. 5, pp. 467-476.
- [3] O’Connor, P. and Kleyner, A. (2012) *Practical Reliability Engineering*. Chichester, UK: John Wiley & Sons.
- [4] IEEE 1856/D33 (2017), Draft Standard Framework for Prognosis and Health Management (PHM) of Electronic Systems, Mar 2017.
- [5] CAVE3 (Accessed 2015, Nov.) Prognostics Health Management for Electronics, Auburn University, Auburn, Alabama. Web site: <http://cave.auburn.edu/rsrch-thrusts/prognostic-health-management-for-electronics.html>.
- [6] Hofmeister, J., Wagoner, R. and Goodman, D. (2013) “Prognostic Health Management (PHM) of Electrical Systems using Conditioned-based Data for Anomaly and Prognostic Reasoning,” *Chemical Engineering Transactions*, Vol. 33, pp. 992-996.
- [7] Hofmeister, J. Szidarovszky, F. and Goodman, D. (2017) “An Approach to Processing Condition-based Data for Use in Prognostic Algorithms,” 2017 Machine Failure Prevention Technology, Virginia Beach, VA, 15-18 May 2017.
- [8] Medjaher, K. and Zerhouni, N. (2013) “Framework for a Hybrid Prognostics,” *Italian Association of Chemical Engineering, Chemical Engineering Transactions*, DOI: 10.3303/CET1333016, pp. 91-96, 2013.
- [9] Erickson, R. (1999), *Fundamentals of Power Electronics*, Norwell, MA: Kluwer Academic Publishers.
- [10] Judkins, J. B., Hofmeister, J. and Vohnout, S. (2007) “A Prognostic Sensor for Voltage Regulated Switch-Mode Power Supplies,” IEEE Aerospace Conference 2007, Big Sky, MT, 4-9 Mar. 2007, Track 11-0804, pp. 1-8.
- [11] Judkins, J. B. and Hofmeister, J. P. (2007) “Non-invasive Prognostication of Switch Mode Power Supplies with Feedback Loop Having Gain,” IEEE Aerospace Conference 2007, Big Sky, MT, 4-9 Mar. 2007.
- [12] Hofmeister, J. Goodman, D. and Wagoner, R. (2016) “Advanced Anomaly Detection Method for Condition Monitoring of Complex Equipment and Systems,” 2016 Machine Failure Prevention Technology, Dayton, OH, 24-26 May 2016.
- [13] TI (1995) “Understanding Data Converters,” Application Report SLAA013, Texas Instruments, Inc., 1999.
- [14] Carr, J.J. and Brown, J.M. (2000), *Introduction to Biomedical Equipment Technology*, 4<sup>th</sup> Ed., Upper Saddle River, New Jersey, Prentice Hall
- [15] Jenq, Y.C. and Li, Qiong, (2002) “Differential Non-linearity, Integral Non-Linearity, and Signal to Noise Ratio of an Analog to Digital Converter,” Department of Electrical and Computer Engineering, Portland State University, P.O. Box 751, Portland, OR. 97207, USA.

## BIOGRAPHY



**James Hofmeister** has a B.S. in Electrical Engineering from the University of Hawai'i, Honolulu, Hawai'i and an M.S. in Electrical and Computer Engineering from the University of Arizona, Tucson, Arizona. After a 30-year career with IBM and five years of

retirement, he joined Ridgetop Group, Inc. in 2003. He is currently a distinguished engineer in research and product development and specializes in many areas of engineering, including microelectronics, radiation-hardening, mixed-signal circuits and sensors, and support for diagnostics and prognostic health monitoring/management systems. His accomplishments include seven issued U.S. patents and over 30 published papers and articles. He is currently an IEEE life member and a member of the Board of Directors of the Machinery Failure Prevention Technology conference, where he is chair of the Sensors Focus Group.



**Ferenc Szidarovszky** received a BS, an MS and a PhD in mathematics from the Eotvos University of Sciences of Budapest, Hungary. He is also a recipient of another PhD from the Budapest University of Economic Sciences. Before emigrating to the USA in 1987

he was a professor of several Hungarian universities. In the USA he has been a professor of systems and industrial engineering at the University of Arizona. After retiring from the U of A in 2011 he became a senior researcher with ReliaSoft Corporation. He joined Ridgetop Group in 2015 where he is senior researcher.



**Doug Goodman** received a B.S. in Electrical Engineering from California Polytechnic State University in San Luis Obispo and an MBA from the University of Portland. Mr. Goodman is accustomed to pioneering innovative electronic technology and establishing engineering

milestones, Mr. Goodman's comprehensive background encompasses low-noise instrumentation, design-for-test (DFT), fault simulation techniques, and design tool development at established firms such as Tektronix and Honeywell where he started his career designing instrumentation and flight control electronics.. As a Vice President, he successfully steered engineering at Analogy Inc., working on electromechanical design simulation tools, until its IPO. This experience inspired him to co-found and head Opmaxx Inc., a design-for-test IP firm that later merged with Credence Systems; and in 2000, he founded Ridgetop Group.